HYPERSPECTRAL MONITORING BASED ON THE NET PHOTOSYNTHETIC RATE OF BROOMCORN MILLET UNDER VARYING PHOTOPERIODS

LI, R.[2] – CHANG, B.[2] – CUI, X. Y.[2] – DAI, C. Y.[2] – TIAN, X.[1] – CHEN, L.[1] – QIAO, Z. J.[1] – WANG, J. J.[1*]

[1]*Center for Agricultural Genetic Resources Research, Shanxi Agricultural University/Key Laboratory of Crop Gene Resources and Germplasm Enhancement on Loess Plateau, Ministry of Agriculture, Taiyuan, China*

[2]*College of Agriculture, Shanxi Agricultural University, Taigu, China (phone: +86-175-5027-8898)*

[*]*Corresponding author e-mail: xiaoleiwangjie@163.com; phone: +86-152-3404-0919*

(Received 2nd Apr 2025; accepted 11th Jun 2025)

Abstract. Photoperiod regulates photosynthetic electron transport and influence carbon assimilation in broomcorn millet. This study employed hyperspectral technology to decode coupling mechanisms of photoperiod-net photosynthetic rate (Pn) using light-sensitive (LM5) and light-insensitive (YR01) cultivars under three treatments: natural light (CK), short-day treatment before heading (G1/G2), and short-day treatment throughout the growth period (G3). Pn prediction models were constructed using partial least squares (PLS), support vector machine (SVM), and back-propagation neural network (BPNN). Results showed that G3 increasing Pn by 15.76% (LM5) and 5.58% (YR01) ($P<0.05$). The 1ST treatment exhibited the best correlation between the spectral data and Pn ($r = -0.535$), with the 1ST-RSI (716, 715 nm) showing the highest correlation ($r = 0.658$). The full-spectrum PLS model showed superior performance (validation $R^2=0.669$, RMSE=3.226, RPD=1.642). These findings confirm that the synergistic optimization of spectral preprocessing and modeling algorithms can precisely quantify the photoperiodic response of broomcorn millet Pn, providing technical support for the application of hyperspectral technology in assessing photosynthetic productivity and guiding crop management.
Keywords: *broomcorn millet, photoperiod, net photosynthetic rate, spectral index, SVM, PLS, BPNN*

Introduction

Broomcorn millet (*Panicum miliaceum* L.) is a minor cereal crop known for its tolerance to poor soils and drought conditions (Feng et al., 2019). Its cultivation originates from Northern China, and its cultivation history spans over 10,000 years (Loukas et al., 2009). Photosynthesis is a critical physiological process in plant growth and development, and the net photosynthetic rate (Pn) is an important parameter characterizing the strength of photosynthesis. Leaf Pn is closely related to intrinsic factors such as chlorophyll content and leaf maturity, and is also affected by environmental factors like light intensity and relative humidity (Zhang et al., 2006; Jiang et al., 2015; Guan et al., 2024). Photoperiod is one of the most important environmental factors influencing flowering (Liu et al., 2024). It modulates photoreceptor signal transduction pathways, dynamically adjusting the electron transport efficiency of photosystem II (PSII) and Rubisco enzyme activity, which in turn determines the spatiotemporal variation of leaf Pn. As a short-day crop, broomcorn millet is extremely sensitive to changes in photoperiod (Wang et al., 2020a), and differences in photoperiod response thresholds among cultivars directly affect population-level photosynthetic efficiency and yield composition.

http://www.aloki.hu ● ISSN 1589 1623 (Print) ● ISSN1785 0037 (Online)
DOI: http://dx.doi.org/10.15666/aeer/2304_78557871

Traditional methods for obtaining photosynthetic parameters mainly rely on single-leaf, in vitro measurements using portable photosynthesis systems such as the CI-340 (Yao et al., 2009) and LI-6400 (Dou et al., 2021). Although these methods can accurately capture instantaneous Pn values, they are limited by a lack of sample representativeness, destructive sampling, and difficulties in dynamic monitoring at the population scale. Hyperspectral technology, with its nanometer-level spectral resolution and continuous wavelength coverage, offers a powerful approach to measure plant traits simultaneously, accurately, and rapidly across different spectral bands. This technique provides abundant spectral information and offers a novel method for rapid, large-scale evaluation of crop photosynthetic efficiency (Du et al., 2024; Di et al., 2024; Zhang et al., 2024; Huo et al., 2024).

At present, three common approaches are used to construct spectral monitoring models. The first approach employs full-spectrum methods. For example, Wang et al. (2019) used stepwise multiple linear regression, PLS, and SVM to construct models for monitoring broomcorn millet leaf nitrogen content and grain protein content based on the full spectrum, with the SVM model performing best. The second approach utilizes feature wavelengths to construct monitoring models. For instance, Liang et al. (2024) applied convolutional neural networks (CNN) based on both the full spectrum and feature wavelengths to identify different disease severities of early blight in potatoes, and found that the CNN model using first derivative spectra reduced by a random frog (RF) algorithm achieved the highest overall accuracy of 91.18%. The third approach constructs monitoring models using spectral indices. For example, Tang et al. (2024) built a soybean yield estimation model using seven spectral indices as independent variables, and found that the FDmSR index during the full pod stage had the highest correlation with yield ($r = 0.717$).

In recent years, many scholars have conducted extensive research on the remote sensing monitoring of Pn. Yan (2023a) demonstrated that short-day treatment before heading significantly increased the Pn of broomcorn millet. Jing et al. (2023) found that in Ningxia foxtail millet, as photoperiod extended, antioxidant enzyme activity first decreased and then increased, while chlorophyll content and Pn exhibited opposite trends. Wang et al. (2016) analyzed the relationships between vegetation spectral indices (VI), photosynthetically active radiation (PAR), and Pn, concluding that the CIredge*PAR index was optimal for constructing an inversion model of Pn. Wang et al. (2020b) constructed a Pn prediction model based on spectral indices derived from wavelet transformation, which achieved higher accuracy than models based on sensitive wavelengths. Liu et al. (2020) used rice leaf spectra and photosynthetically active incident radiation to build Pn estimation models under different nitrogen levels for various rice cultivars, and verified that the vegetation index CI provided the best inversion results, with R^2 values exceeding 0.75 and RMSE not exceeding 1.85. Zhang et al. (2022) demonstrated that a novel composite index constructed from remote sensing vegetation indices (VIs) and solar-induced chlorophyll fluorescence (SIF) could significantly improve the inversion accuracy of Pn in young rapeseed seedlings. Wu et al. (2023) showed that integrating gradient boosting decision trees (GBDT) and random forest (RF) models with combined inputs enabled precise monitoring of rice Pn.

However, few studies have addressed the spectral response mechanism and monitoring model of broomcorn millet Pn under photoperiod regulation. As a pioneer crop in earthquake relief, broomcorn millet is often planted as a post-disaster remedy crop, and its sowing dates are significantly different. With the delay of the sowing date, the duration

http://www.aloki.hu ● ISSN 1589 1623 (Print) ● ISSN1785 0037 (Online)
DOI: http://dx.doi.org/10.15666/aeer/2304_78557871

of photoperiod during the growing season gradually shortens. How to achieve the coordinated regulation of shortening the growth period and maintaining the yield under short-day conditions, and then optimize field management through early remote sensing monitoring, is an important scientific issue in broomcorn millet production. Therefore, conducting remote sensing monitoring research under short-day conditions is of great theoretical significance and practical value for revealing the photoperiod response mechanism of broomcorn millet and screening photoperiod-optimized varieties to adapt to the light resource characteristics of different planting areas. In this study, two broomcorn millet cultivars with marked differences in photoperiod sensitivity, LM5 and YR01, were used as materials. Four photoperiod treatments were applied: natural light throughout the growth period (CK), short-day treatment before heading (G1), short-day treatment after heading (G2), and short-day treatment during the entire growth period (G3). The spatiotemporal variation of Pn under these different treatments was systematically analyzed. Raw spectral data were preprocessed using a combination of SG and 1ST transformation, and Pn prediction models were constructed based on full-spectrum, feature wavelengths, and optimized spectral indices (NDSI, RSI, DSI) using machine learning methods (SVM, PLS, and BPNN). Model performance was comprehensively evaluated using the coefficient of determination (R^2), root mean square error (RMSE), and relative prediction deviation (RPD). The results of this study will elucidate the coupling mechanism among photoperiod, spectral response, and Pn, and provide a novel spectral diagnostic model for remote sensing monitoring of broomcorn millet photosynthetic productivity. These findings hold significant practical value for optimizing photoperiod management strategies and developing precise cultivation practices.

Materials and methods

Experimental design

The experiment was conducted at Dingxiang County, Xinzhou City, Shanxi Province， China (38°33′N, 112°54′E). The experimental site is at an altitude of 780 m and falls within a temperate continental monsoon climate zone, with an average annual precipitation of 413-430 mm, an average annual temperature of 8.7 °C, and a frost-free period of 150 days. When conducting the broomcorn millet pot experiment outdoors in this study, to ensure suitable growth conditions: in terms of temperature, the germination period was 15-25℃, the growth period was 20-35℃, and photoperiod regulation was initiated at the seedling stage; Regarding the soil, the tested soil was taken from the 0-20 cm cultivated layer of the field and no fertilizers were applied. In terms of water management, maintain moisture during the germination period, keep the soil moist during the growth period when it is dry, and increase water supply during the Heading stage. Use the soil moisture rapid measurement instrument (OK-S3 type produced by Zhengzhou Oukeqi Instrument Manufacturing Co., LTD.) to monitor the soil moisture content in real time. When the moisture content is lower than 60% of the field capacity, carry out quantitative water replenishment (1 L each time). In terms of pot management, in this experiment, POTS with a specification of 25 cm (height diameter) ×20 cm (base diameter) ×30 cm (diameter) were selected.

The experimental materials consisted of two genotypes with marked differences in photoperiod and temperature sensitivity: the light-sensitive Material LM5 (L) and the

http://www.aloki.hu ● ISSN 1589 1623 (Print) ● ISSN1785 0037 (Online)
DOI: http://dx.doi.org/10.15666/aeer/2304_78557871

light-insensitive Material YR01 (Y). Seeds were sown on June 14, 2022, with 20 seeds per pot and five biological replicates per treatment. And all the data were calculated based on five biological replicates. Four photoperiod treatments were designed (*Table 1*). After the seedlings emerged, thinning was conducted to maintain 10 uniformly growing seedlings per pot. Photoperiod regulation was initiated at the three-leaf stage and the treatment was terminated after the collection of relevant data at the mature stage. In the short-day treatment group, the photoperiod was set to 12 hours (natural light from 07:00 to 19:00, with shading in a dark room from 19:00 to 07:00 the following day).

Table 1. *Different photoperiod treatments in the experiment*

Treatment	Photoperiodic treatment	
	Trefoil stage-Heading period	**Heading period-Mature period**
L-CK	Natural light	Natural light
L-G1	Natural light	Short days
L-G2	Short days	Natural light
L-G3	Short days	Short days
Y-CK	Natural light	Natural light
Y-G1	Natural light	Short days
Y-G2	Short days	Natural light
Y-G3	Short days	Short days

Note: *Table 1* Photoperiod treatment designs for LM5 and YR01 at different growth stages. L: indicates light-sensitive material, Y: indicates light-insensitive material; CK: natural light throughout the growth period; G1-G3 are experimental groups: G1 (short-day treatment before heading), G2 (short-day treatment after heading), G3 (short-day treatment during the entire growth period)

Measurement methods and techniques

Spectral measurement

A FieldSpec4 portable field hyperspectral radiometer (Sun et al., 2020) was used for spectral measurements. This instrument, manufactured by ASD (Analytical Spectral Devices, Inc., USA), is designed for measuring and analyzing spectra in field environments (*Figure 1*). The ASD spectrometer covers a wavelength range of 350-500 nm, with a spectral resolution of 3 nm (350-1000 nm) and 10 nm (1000-2500 nm). Its scanning time is 100 ms, with spectral sampling intervals of 1.4 nm (350-1000 nm) and 2 nm (1000-2500 nm), and a wavelength accuracy of ±1 nm. A PTFE standard white panel (Sun et al., 2016) was used as the standard reference. Canopy measurements of broomcorn millet were conducted between 10:00 and 14:00 under clear, calm, or light wind conditions. Measurements were performed starting at the flowering stage and then at 7-day intervals, specifically at the flowering stage, 7, 14, 21, and 28 days after flowering, and at maturity. During measurement, the probe was aimed directly at the canopy, and the measurement button was pressed to begin data acquisition.

Pn measurement

Simultaneously with the canopy spectral measurements, the Pn was measured on the inverted second leaves of broomcorn millet using a CI-340 (CID Bio-Science, Inc., USA) portable photosynthesis system (*Figure 2*). For each measurement, four plants were sampled, and each plant was measured three times; the average value was then calculated. These measurements were typically conducted between 9:00 and 11:00 in the morning under clear and calm (or light wind) conditions.

http://www.aloki.hu ● ISSN 1589 1623 (Print) ● ISSN1785 0037 (Online)
DOI: http://dx.doi.org/10.15666/aeer/2304_78557871

Figure 1. *The FieldSpec 4 portable spectrometer*

Figure 2. *The CI-340 portable photosynthesis meter*

Spectral index calculation

Three optimized spectral indices were selected for constructing the Pn prediction model (*Table 2*): The Normalized Difference Spectral Index (NDSI) (Gao et al., 2025), the Difference Spectral Index (DSI), and the Ratio Spectral Index (RSI) (Fu et al., 2024).

Table 2. *Spectral indices and their calculation formulas*

Spectral parameter	Name	Formula	References
NDSI	Normalized interpolation index	$(R_{\lambda1}- R_{\lambda2})/(R_{\lambda1}+ R_{\lambda2})$ (Eq.1)	Gao et al. (2025)
DSI	Difference Spectral Index	$R_{\lambda1}- R_{\lambda2}$ (Eq.2)	Fu et al. (2024)
RSI	Ratio spectral index	$R_{\lambda1} / R_{\lambda2}$ (Eq.3)	Fu et al. (2024)

Note: λ1 and λ2 represent random wavelengths in the range of 400 to 2500 nm. (This table shows the spectral indices used in this study and their calculation formulas. Spectral indices are calculated by combining and comparing spectral characteristics across different wavelength ranges, which are used to characterize surface cover types, crop growth conditions, soil properties)

http://www.aloki.hu ● ISSN 1589 1623 (Print) ● ISSN1785 0037 (Online)
DOI: http://dx.doi.org/10.15666/aeer/2304_78557871

Model construction and evaluation

In this study, models were developed using Support Vector Machines (SVM), Partial Least Squares (PLS), and Back-propagation (BPNN). The model accuracy was evaluated using statistical parameters including R^2, RMSE, and RPD. A higher R^2 (closer to 1) and lower RMSE indicate better model prediction accuracy (Li et al., 2018). Generally, an RPD value below 1.5 indicates unsatisfactory accuracy; 1.5 ≤ RPD < 2 suggests good predictive accuracy; and RPD ≥ 2 implies excellent predictive capability for the sample data (Li et al., 2024a). The calculation formulas are as follows:

$$R^2 = \frac{\sum_{i=1}^{n}(Y_i' - \bar{Y}_i)^2}{\sum_{i=1}^{n}(Y_i - \bar{Y}_i)^2} \quad \text{(Eq.4)}$$

$$RMSE = \sqrt{\frac{1}{n}\sum_{i=1}^{n}(Y_i - Y_i')^2} \quad \text{(Eq.5)}$$

$$RPD = \frac{SD}{RMSE} \quad \text{(Eq.6)}$$

In the formula, n represents the number of samples, Y_i' and Y_i are the predicted and actual values of the samples respectively, $\bar{Y}_i$ is the mean of the actual sample values, and SD is the standard deviation of the samples.

Data processing

The collected data were processed using Excel 2019, and statistical analyses of the experimental data were performed with SPSS 26. PLS, SVM, and BPNN models were constructed using Matlab 2010 and Matlab 2022, respectively. The raw spectral data were preprocessed using 1ST and SG smoothing in Unscrambler X 10.4, and plotting and analysis were carried out using Origin 2021.

Results and discussion

Descriptive statistics

A total of 144 broomcorn millet leaf Pn samples were collected. The samples were sorted from low to high using a concentration gradient method and then divided into a modeling set and a validation set in a 3:1 ratio. As shown in the table (*Table 3*), the variation range of Pn in both groups is similar, with a relatively large overall range, and the mean values of the modeling and validation sets are close. Overall, these results indicate that the division of the modeling and validation sets is reasonable and suitable for model construction and validation.

Table 3. *Descriptive statistical analysis of Pn of broomcorn millet leaves*

Data set	Sample size	Total distance	Mix	Max	Mean	SD	Variance
Modeling set	108	21.430	1.770	23.20	13.111	5.264	27.712
Validation set	36	20.37	2.28	22.65	13.186	5.298	28.072

Note: The variance, minimum value(Mix), maximum value(Max), mean, and standard deviation(SD) are $\mu mol \cdot m^{-2} \cdot s^{-1}$

http://www.aloki.hu ● ISSN 1589 1623 (Print) ● ISSN1785 0037 (Online)
DOI: http://dx.doi.org/10.15666/aeer/2304_78557871

Analysis of spectral characteristics related to Pn in broomcorn millet leaves

Based on the spectral data at the flowering stage for LM5 and YR01, this study preprocessed the data by excluding the 1801-1949 nm range (which is subject to abnormal fluctuations due to interference from atmospheric water vapor absorption bands). Under different photoperiod treatments, significant differences in spectral reflectance were observed between the two materials in the 700–1350 nm range (*Figure 3*). In the pre-heading natural light treatment groups (CK and G1), reflectance was generally higher than that in the short-day treatment groups (G2 and G3). After heading, the LM5 material exhibited a reflectance gradient of L-G1 > L-CK > L-G3 > L-G2, whereas YR01 showed a gradient of Y-CK > Y-G1 > Y-G2 > Y-G3, indicating that broomcorn millet genotypes with different light sensitivities display distinct response mechanisms to photoperiod changes.

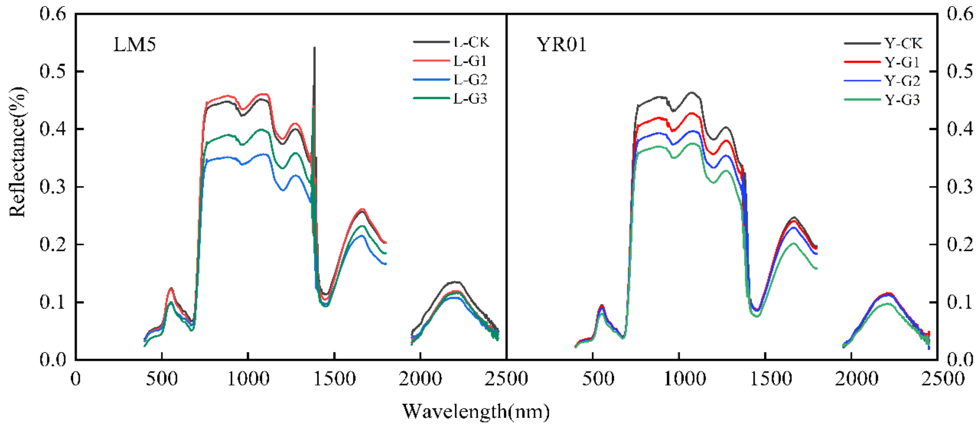

Figure 3. *Spectral reflectance curve of broomcorn millet leaves (flowering Stage). (The figure shows the spectral reflection characteristics of broomcorn millet leaves at flowering stage under different photoperiod treatment. The abscissa represents the wavelength (nm), and the ordinate represents the spectral reflectance, L and Y represent the light-sensitive material LM5 and the light-insensitive material YR01 respectively)*

Analysis of the near-infrared band (750-1350 nm) across six developmental stages for the two materials (*Figure 4*) showed that LM5 reached its reflectance peak (0.430) 7 days after flowering, while YR01 achieved its highest reflectance (0.415) during the flowering stage. At maturity, the full-spectrum reflectance of both materials dropped to the lowest values, which may be closely related to the disintegration of chloroplast structures and a reduction in chlorophyll content, as well as decreased tissue moisture during leaf senescence.

Effects of different treatments on the Pn of broomcorn millet

As shown in *Figure 5*, the two materials generally exhibit a parabolic trend in Pn with advancing growth stages. Both YR01 (except under the G1 treatment) and LM5 reach their maximum Pn 14 days after flowering. Specifically, YR01 under CK, G2, and G3 treatments shows maximum Pn values of 19.7, 20.23, and 20.80 μmol m^{-2} s^{-1}, respectively, with the ranking G3 > G2 > CK (*Figure 5A*). In contrast, LM5 displays maximum Pn values of 17.7, 20.23, 22.38, and 20.49 μmol m^{-2} s^{-1} under CK, G1, G2, and G3 treatments,

http://www.aloki.hu ● ISSN 1589 1623 (Print) ● ISSN1785 0037 (Online)
DOI: http://dx.doi.org/10.15666/aeer/2304_78557871

respectively, with the order G2 > G3 > G1 > CK (*Figure 5B*), indicating that short-day treatment before heading can significantly enhance the photosynthetic efficiency of LM5.

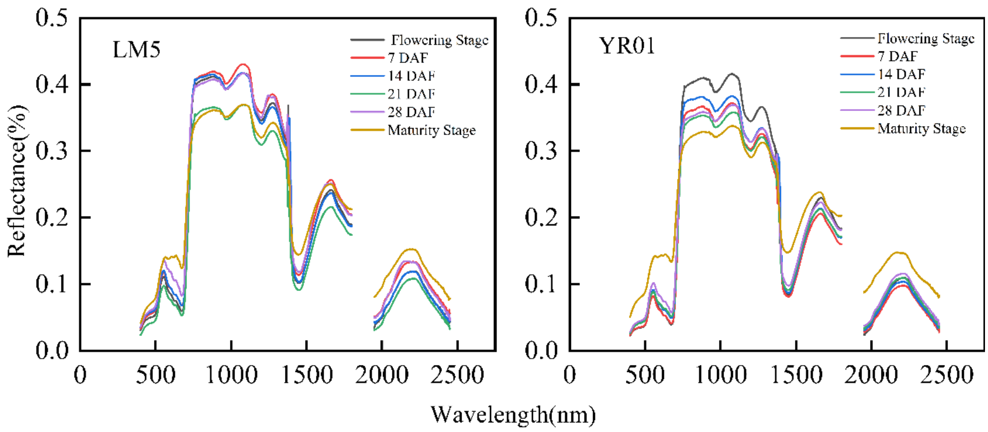

***Figure 4.** Spectral reflectance curve of broomcorn millet leaves at different periods. (The figure shows the dynamic changes of spectral reflectance of two kinds of broomcorn millet materials at different growth stages. The abscissa represents the wavelength (nm), and the ordinate represents the spectral reflectance, the curves of different colors represent the spectral reflectance of LM5 and YR01 at the flowering stage, 7 days after flowering(7DAF), 14 days after flowering(14DAF), 21 days after flowering(21DAF), 28 days after flowering(28DAF), and mature stage respectively)*

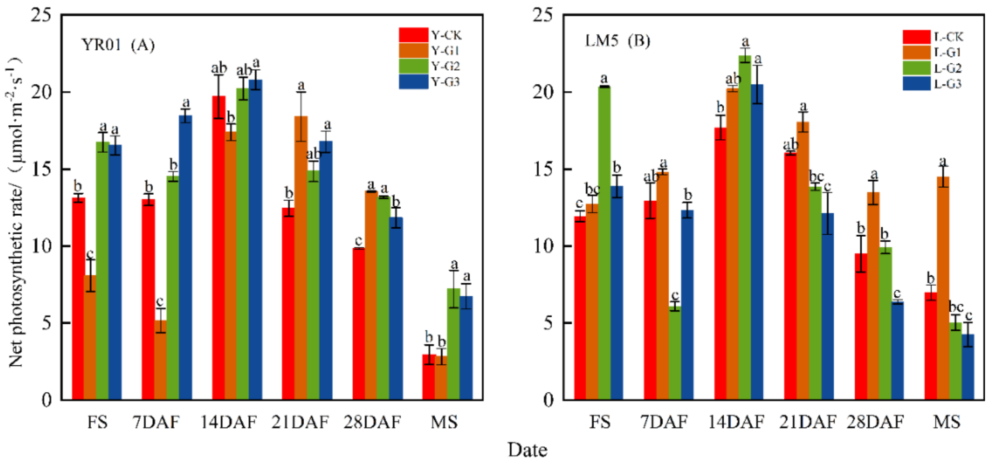

***Figure 5.** Effects of different treatments on Pn of broomcorn millet leaves. Note: Different lowercase letters indicate the significance of different treatments at the level of 0.05(independent sample t-test, *p < 0.05). (Flowering Stage (FS); 7 Days After Flowering (7 DAF); 14 Days After Flowering (14 DAF); 21 Days After Flowering (21 DAF); 28 Days After Flowering (28 DAF); Maturity Stage (MS))*

Across different growth stages, the Pn values of both materials vary markedly under different light treatments. For YR01, the Pn under full-period short-day treatment (G3) is significantly higher than that under natural light (CK) throughout the growth period, with increases of 25.9%, 41.80%, 5.57%, 34.73%, 20.29%, and 128.99% relative to CK, respectively. In contrast, for LM5, the Pn under G3 is significantly lower than that under

http://www.aloki.hu ● ISSN 1589 1623 (Print) ● ISSN1785 0037 (Online)
DOI: http://dx.doi.org/10.15666/aeer/2304_78557871

CK (except at the flowering stage and 14 days after flowering), with decreases of 4.81%, 24.46%, 32.74%, and 39.09% relative to CK. These results indicate that the Pn of YR01 is less affected by short-day conditions.

When comparing the Pn between the pre-heading short-day treatment (G1) and the full-period natural light (CK), LM5 under G1 exhibits a higher Pn than under CK at all growth stages, whereas for YR01, only the 21- and 28-day post-flowering stages show higher Pn under G1 than CK. Furthermore, except for 7, 14, and 21 days after flowering, YR01 under the pre-heading short-day followed by natural light treatment (G2) exhibits a higher Pn than under the full-period short-day treatment (G3), with increases of 1.19%, 11.14%, and 6.87%, respectively (*Figure 5A*). In contrast, LM5 under G2 is higher than under G3 (except at 7 days after flowering) by 46.53%, 9.27%, 14.43%, 55.24%, and 18.38%, respectively (*Figure 5B*). This further confirms that the Pn of YR01 is less sensitive to short-day conditions.

In addition, except at 21 and 28 days after flowering, YR01 under the pre-heading short-day followed by natural light treatment (G2) shows a Pn that is higher than that under the pre-heading natural light followed by short-day treatment (G1) by 107.01%, 181.03%, 16.31%, and 155.44%, respectively (see *Figure 5A*). In contrast, LM5 under G2 is lower than under G1 (except during the flowering stage and 14 days after flowering) by 58.88%, 23.20%, 26.39%, and 65.29%, respectively (*Figure 5B*). These findings indicate that for YR01, the pre-heading short-day treatment exerts a greater effect on Pn than the short-day treatment applied after heading, whereas LM5 exhibits the opposite trend.

An average analysis of Pn over the entire growth period for both materials revealed that under the CK treatment, differences in Pn between the materials were not significant (*Figure 6*), although LM5 exhibited a higher Pn than YR01. Under the G1 treatment, however, LM5’s Pn was significantly higher than that of YR01, whereas under the G2 and G3 treatments, LM5’s Pn was significantly lower than YR01’s. These results indicate that the response mechanisms to photoperiod variations differ markedly between genotypes with different light sensitivities.

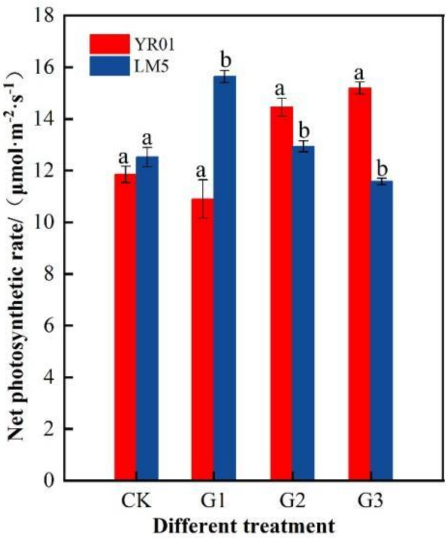

Figure 6. *Effects of different treatments on Pn of broomcorn millet leaves. Note: Different lowercase letters indicate the significance of different treatments at the level of 0.05(independent sample t-test, *p < 0.05)*

http://www.aloki.hu ● ISSN 1589 1623 (Print) ● ISSN1785 0037 (Online)
DOI: http://dx.doi.org/10.15666/aeer/2304_78557871

Correlation analysis between broomcorn millet leaf net Pn and canopy spectral reflectance under different preprocessing methods

In this study, the raw spectral reflectance (R) of broomcorn millet was preprocessed using both 1ST and SG smoothing techniques, and their correlations with Pn were analyzed. As shown in *Figure 7*, after preprocessing, the SG-processed reflectance exhibited a trend consistent with the raw reflectance, whereas the 1ST reflectance displayed marked differences compared to R. Over the full spectral range, the correlation between the preprocessed reflectance (using both 1ST and SG methods) and Pn fluctuated between positive and negative values. Notably, the 1ST-preprocessed reflectance exhibited the highest correlation with Pn, with a correlation coefficient of -0.535.

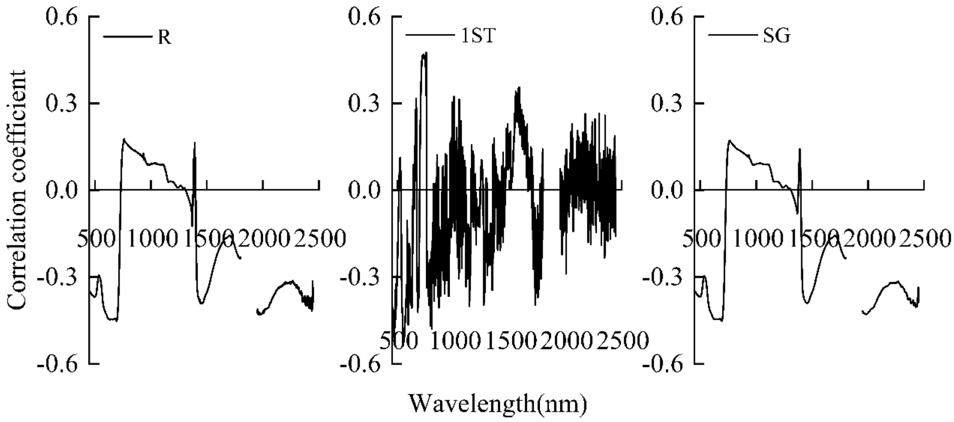

Figure 7. *Correlation between spectral reflectance of leaf canopy and Pn of broomcorn millet after different pretreatment. (The figure presents the correlation analysis results between the spectral reflectance after preprocessing and the Pn of broomcorn millet. The abscissa is the wavelength (nm), and the ordinate is the correlation coefficient. R represents original spectral reflectance, SG represents Savitzky Golay smoothing, 1ST represents first derivative)*

Screening of optimal spectral indices

In this study, an exhaustive search was conducted to calculate the correlations between all possible combinations of optimized spectral indices (RSI, NDSI, DSI) and the Pn of broomcorn millet leaves (*Figure 8*). As shown in the table (*Table 4*), the 1ST-RSI (716, 715) derived from 1ST preprocessing exhibited the highest correlation with Pn, with a correlation coefficient of 0.658. When using the 1ST-RSI spectral index to construct a Pn monitoring model for broomcorn millet, the modeling set yielded an R^2 of 0.341, an RMSE of 13.182, and an RPD of 0.399, while the validation set produced an R^2 of 0.181, an RMSE of 13.245, and an RPD of 0.40.

Determination of feature wavelengths for Pn

Based on the Successive Projections Algorithm (SPA) analysis, 1950 nm and 1393 nm were identified as the characteristic wavelengths from the raw spectral data. In contrast, the 1ST-preprocessed spectra yielded feature wavelengths of 485 nm, 830 nm, 2005 nm, 1032 nm, and 1361 nm, and the SG-smoothed spectra produced feature wavelengths of 685 nm and 1390 nm. These wavelengths were subsequently used for the construction of feature-based models (*Table 5*).

http://www.aloki.hu ● ISSN 1589 1623 (Print) ● ISSN1785 0037 (Online)
DOI: http://dx.doi.org/10.15666/aeer/2304_78557871

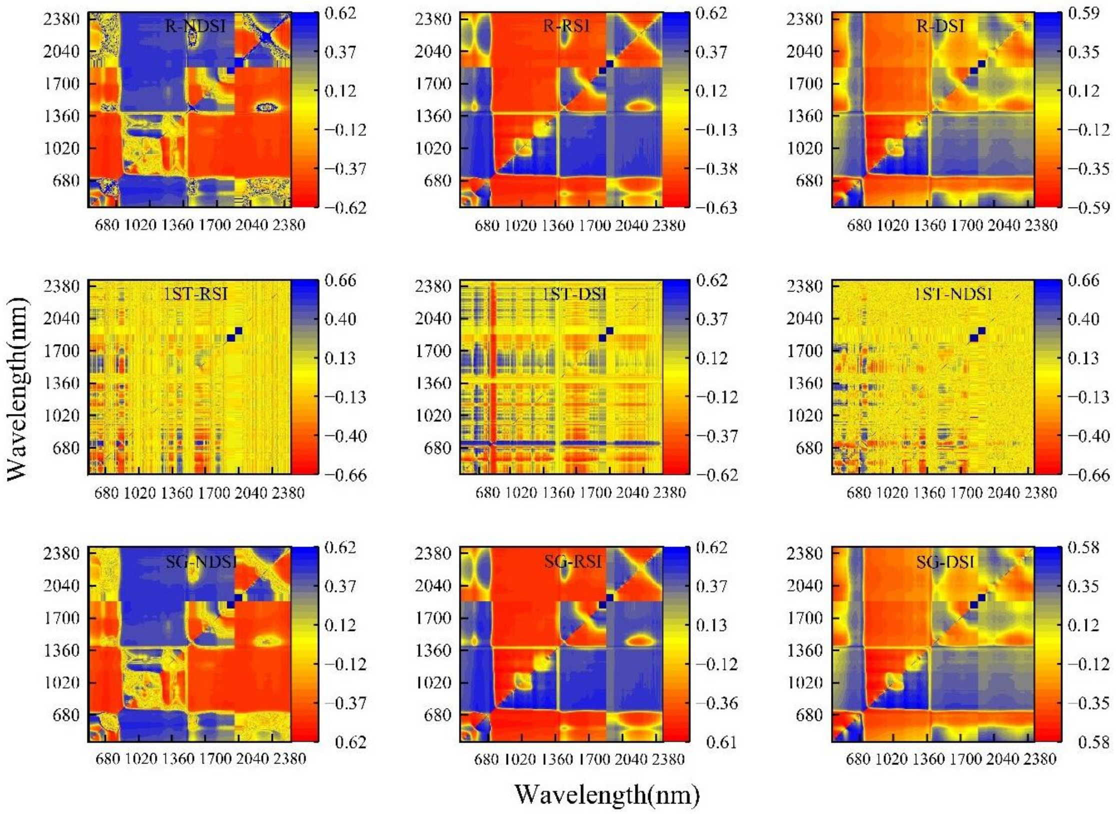

Figure 8. *Correlation coefficient between the dual-band random combination spectral index and the Pn of broomcorn millet leaves. (The figure shows the correlation coefficient plots between dual - band spectral indices and the Pn of broomcorn millet. The abscissa is the wavelength (nm), and the ordinate is the correlation coefficient. The curves of different colors represent the correlations between different dual - band spectral indices (RSI, NDSI, DSI,) constructed from the original spectral reflectance (R), SG - preprocessed reflectance, and 1ST - preprocessed reflectance and Pn)*

Table 4. *Optimum spectral bands and correlation coefficients*

Spectral index	Calculation formula	Wavelength/nm	Correlation coefficient
R-DSI		(549,553)	0.585
1ST-DSI	$R_{\lambda1}$- $R_{\lambda2}$	(495,548)	0.620
SG-DSI		(531,569)	0.579
R-NDSI		(527,571)	0.618
1ST-NDSI	$(R_{\lambda1}-R_{\lambda2})/(R_{\lambda1}+R_{\lambda2})$	(552,1761)	0.657
SG-NDSI		(527,572)	0.617
R-RSI		(2204,2172)	0.620
1ST-RSI	$R_{\lambda1}/R_{\lambda2}$	(716,715)	0.658
SG-RSI		(529,572)	0.611

Note: The table shows the optimal spectral bands constructed based on different preprocessed spectral reflectances and their correlation coefficients with the Pn of broomcorn millet. The study calculated the correlations between all possible combinations of spectral indices and the Pn of broomcorn millet to screen out the optimal spectral bands

http://www.aloki.hu ● ISSN 1589 1623 (Print) ● ISSN1785 0037 (Online)
DOI: http://dx.doi.org/10.15666/aeer/2304_78557871

Table 5. *Fitting of hyperspectral model of Pn of broomcorn millet leaves*

	Model type	Calibration			Validations		
		R^2	RMSE	RPD	R^2	RMSE	RPD
Characteristic band	R-BP	0.340	4.259	1.236	0.053	5.356	0.989
	1ST-BP	0.263	4.615	1.141	0.121	5.126	1.034
	SG-BP	0.294	4.538	1.160	0	6.193	0.856
	R-PLS	0.264	4.495	1.171	0.190	4.775	1.110
	1ST-PLS	0.205	4.673	1.126	0.069	5.198	1.019
	SG-PLS	0.289	4.419	1.191	0.225	4.748	1.116
	R-SVM	0.260	4.529	1.162	0.178	4.876	1.087
	1ST-SVM	0.525	3.966	1.327	0.119	4.937	1.073
	SG-SVM	0.312	4.259	1.211	0.083	5.018	1.056
Full band	R-BP	0.105	6.979	0.754	0.010	7.772	0.682
	1ST-BP	0.701	2.927	1.799	0.226	5.082	1.043
	SG-BP	0.583	3.609	1.459	0.276	5.385	0.984
	R-PLS	0.884	1.786	2.947	0.415	4.141	1.279
	1ST-PLS	0.906	1.606	3.278	0.669	3.226	1.642
	SG-PLS	0.638	3.154	1.669	0.359	4.303	1.231
	R-SVM	0.559	3.504	1.502	0.212	4.705	1.126
	1ST-SVM	0.994	0.515	10.224	0.615	3.606	1.469
	SG-SVM	0.523	3.624	1.453	0.189	4.806	1.103

Note: The table shows the hyperspectral model fitting of broomcorn millet leaf Pn. In this study, three preprocessing methods based on R, IST, and SG were compared, and three modeling methods including BPNN, PLS and SVM were combined. The evaluation indexes included coefficient of R^2, RMSE and RPD

Construction of hyperspectral models for Pn

Pn monitoring models were developed based on both the full spectrum and selected feature wavelengths. As shown in the table (*Table 5*), the full-spectrum models outperformed those based on feature wavelengths. Among the full-spectrum models, the PLS model performed better than both the BPNN and SVM models, making it the optimal choice. Notably, the 1ST-PLS model achieved superior performance compared to both the R-PLS and SG-PLS models, with training set R^2 of 0.906, validation set R^2 of 0.669, RMSE values of 1.606 and 3.226, and RPD values of 3.278 and 1.642, respectively. These results indicate that the full-spectrum 1ST-PLS model can predict broomcorn millet Pn with greater accuracy.

Evaluation of the accuracy of broomcorn millet Pn monitoring models

In this study, three types of broomcorn millet Pn monitoring models were constructed based on the full spectrum, feature wavelengths, and optimized spectral indices. Among the models built using spectral data preprocessed by the 1ST and SG smoothing methods, the best-performing model was the full-spectrum 1ST-PLS model (R^2 = 0.669; RMSE = 3.226; RPD = 1.642). These results demonstrate that the 1ST spectral preprocessing method substantially enhances model accuracy, and that the PLS model is able to predict broomcorn millet Pn more precisely (*Figure 9*).

http://www.aloki.hu ● ISSN 1589 1623 (Print) ● ISSN1785 0037 (Online)
DOI: http://dx.doi.org/10.15666/aeer/2304_78557871

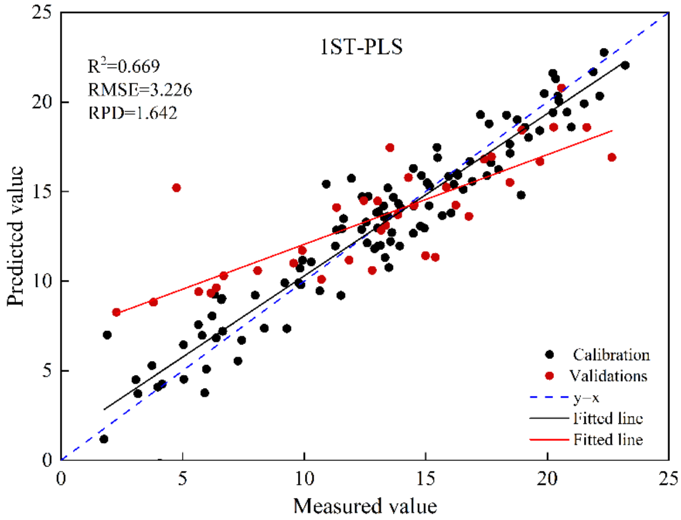

Figure 9. *Broomcorn millet between measured and predicted Pn 1:1 fitting figure. (The figure shows the fitting plots of the Pn optimal models for broomcorn millet. The abscissa represents the measured values, and the ordinate represents the predicted values. The curves of different colors represent the fitting situations of the 1ST - PLS model based on the full spectrum)*

Discussion

Effect of photoperiod on the Pn of broomcorn millet

Photoperiod is one of the critical factors affecting plant growth and development. Our results indicate that photoperiod significantly influences the Pn of broomcorn millet, and the response mechanisms differ markedly between genotypes with different light sensitivities. Short-day treatment before heading significantly increased the leaf Pn in LM5, which is consistent with previous studies in other crops. For example, Li et al. (2024b) found that under a 12 h/12 h photoperiod, cucumber seedlings exhibited significantly greater plant height, stem diameter, and photosynthetic parameters compared to other treatments, indicating that appropriate short-day treatment benefits cucumber photosynthesis. Similarly, Yan (2023a) reported that short-day treatment during the heading stage notably enhanced broomcorn millet Pn. This phenomenon may result from short-day treatment altering the plant's photomorphogenesis, thereby affecting the expression of photosynthesis-related genes and enzyme activities, which in turn promotes photosynthetic processes. For low-sensitivity materials such as YR01, although the impact of short-day treatment on Pn is relatively minor, a certain increase is still observed under the G3 treatment. However, Cai et al. (2024) reported that extending the photoperiod can improve seedling quality, with the highest leaf Pn observed under a 14 h light/10 h dark regimen, which is inconsistent with our findings. This discrepancy suggests that the effect of photoperiod on broomcorn millet Pn is complex and is not only related to species and photoperiod sensitivity but is also subject to comprehensive regulation by other physiological and environmental factors.

Relationship between canopy spectral reflectance and Pn

After preprocessing the R using 1ST and SG methods, the correlation between the spectral reflectance and Pn across the full wavelength range fluctuated between positive and negative values. Among these, the 1ST-preprocessed reflectance exhibited the

http://www.aloki.hu ● ISSN 1589 1623 (Print) ● ISSN1785 0037 (Online)
DOI: http://dx.doi.org/10.15666/aeer/2304_78557871

highest correlation with Pn, reaching -0.535. This finding indicates that the spectral preprocessing method plays a vital role in revealing the intrinsic relationship between the spectral data and Pn. The 1ST method enhances the variability in the spectral curve and accentuates subtle differences in the vegetation spectra, thereby better reflecting changes in the plant's physiological state. Compared with SG, 1ST appears to be more effective in extracting spectral information related to Pn. Similar conclusions have been reached in other crop studies; for instance, in rice and wheat, the 1ST spectral transformation has been widely applied to construct monitoring models for parameters such as photosynthetic rate and chlorophyll content (Luo et al., 2020; Yan et al., 2023b; Thorp et al., 2024). Lü et al. (2017) demonstrated that a QPSR model based on first derivative spectra provided the best analytical model for wheat leaf Pn.

Screening of optimal spectral indices

An exhaustive analysis was performed to calculate the correlation between various combinations of optimized spectral indices (NDSI, DSI, RSI) and broomcorn millet Pn. The analysis revealed that all three spectral indices constructed from 1ST-preprocessed data exhibited correlations with Pn higher than those derived from raw or SG spectra, with all correlations exceeding 0.6. Among them, the 1ST-RSI constructed using wavelengths 716 nm and 715 nm showed the highest correlation with Pn, with a correlation coefficient of 0.658. This result demonstrates that a spectral index based on a specific combination of wavelengths can more effectively capture the variations in Pn. The construction of spectral indices is based on the differential absorption, reflection, and transmission characteristics of plant leaves across various wavelengths, which are closely related to light energy utilization, pigment content, and leaf structure during photosynthesis. In terms of the accuracy of the broomcorn millet Pn monitoring model constructed using these spectral indices, the model based on the optimized 1ST-RSI ($R^2 = 0.181$; RMSE = 13.245; RPD = 0.4) outperformed the DSI and NDSI-based models, indicating a substantial improvement in model accuracy when using 1ST-preprocessed data compared with raw or SG-smoothed reflectance.

Construction and evaluation of hyperspectral models for broomcorn millet Pn

Three types of broomcorn millet Pn hyperspectral monitoring models were developed based on full-spectrum and feature wavelength data using SVM, PLS, and BPNN methods. The results indicate that models constructed using the full spectrum outperformed those based on selected feature wavelengths. The advantage of the full-spectrum approach lies in its ability to utilize all available spectral information, thereby avoiding the potential loss of important data during feature wavelength selection. Among the algorithms tested, the PLS model outperformed the BPNN and SVM models. The PLS model achieves this by comprehensively analyzing the independent and dependent variables, extracting the components most contributory to predicting Pn, and effectively reducing data dimensionality and multicollinearity issues, thereby improving both accuracy and stability. Our results indicate that the 1ST-PLS model is optimal, with an R^2 of 0.906 for the training set and 0.669 for the validation set, RMSE values of 1.606 and 3.226, and RPD values of 3.278 and 1.642, respectively, indicating that this model can reliably predict broomcorn millet Pn. Similar conclusions were drawn in previous studies; for instance, Bai et al. (2018) employed the Successive Projections Algorithm combined with PLS regression to build an estimation model for winter wheat nitrogen content, yielding a validation set R^2 of 0.84, RMSE of 0.21, and RPD greater than 2,

http://www.aloki.hu ● ISSN 1589 1623 (Print) ● ISSN1785 0037 (Online)
DOI: http://dx.doi.org/10.15666/aeer/2304_78557871

indicating good predictive accuracy. Similarly, Han et al. (2023) found that a lightweight gradient boosting machine (LightGBM) model based on the first derivative of hyperspectral data could effectively invert cotton Pn, which is in line with our findings that the 1ST-PLS model can more accurately predict broomcorn millet Pn.

Conclusion

In this study, hyperspectral monitoring models for the Pn of broomcorn millet were developed using various machine learning approaches (PLS, SVM, BPNN) based on raw spectral data (preprocessed by 1ST and SG), spectral indices (DSI, NDSI, RSI), and feature wavelengths. The results indicate that the 1ST-PLS model provides the most accurate prediction of broomcorn millet Pn. This approach partially overcomes the time-consuming and labor-intensive limitations of traditional methods and offers technical support for the application of remote sensing technology in broomcorn millet cultivation management.

Acknowledgements. The work was supported by Science and Technology Support Project for the High-Quality Development of"Featured" and "High-Grade" at Shanxi Agricultural University(TYGC25-83) and Central Guiding Local Science and Technology Development Fund Project(YDZJSX20231A035).

REFERENCES

[1] Bai, L. M., Li, F. L., Chang, Q. R., Zeng, F., Cao, J., Lu, G. X. (2018): Increasing accuracy of hyper-spectral remote sensing for total nitrogen of winter wheat canopy by use of SPA and PLS methods. – Journal of Plant Nutrition and Fertilizers 24(05): 1178-1184.

[2] Cai, Y. Y., Zhu, Z. L., Jia, Z. K., Ma, L. Y., Sang, Z. Y., Wu, N. S., Xu, M. Y., Luo, Q. Q., Deng, W. Z., Wang, J. W. (2024): Effects of photoperiod on leaf nutrition and photosynthetic physiology of Magnolia wufengensis 'Jiaohong 1'. – Non-wood Forest Research 42(01): 189-200+210.

[3] Di, L., Chen, Y., Qiao, Y. L., Qin, D., Miao, Y. H., Sheng, K., Li, L. T., Wang, Y. L. (2024): A study on an accurate modeling for distinguishing nitrogen, phosphorous and potassium status in summer maize using in situ canopy hyperspectral data. – Computers and Electronics in Agriculture 221: 108989.

[4] Dou, P. T., Liu, F. Y., Zhang, C. J., Li, K., Nie, H. J., Li, L. A. (2021): Photosynthetic Physiological Characteristics and Adaptation to Dry and Hot Environment of Different Plants in the Dry-Hot Valley of Honghe. – Journal of Northeast Forestry University 49(07): 56-60+65.

[5] Du, R. Q., Xiang, Y. Z., Zhang, F. C., Cheng, J. Y., Shi, H. Z., Liu, H., Yang, X. F., Ning, Y., Yang, X. Z., Wang, T. Y., Wu, Y. X. (2024): Combing transfer learning with the Optical TRApezoid Model (OPTRAM) to diagnosis small-scale field soil moisture from hyperspectral data. – Agricultural Water Management 298: 108856.

[6] Feng, X. M., Zhang, Y. Q. (2019): Characteristics of protective enzyme activities and lipid peroxidation in broomcorn millet leaves under soil water stress. – Agricultural Research in the Arid Areas 37(01): 200-207.

[7] Fu, Z. H., Li, A. G. (2024): Construction of LMA retrieval model based on optimal spectral index. – Standardization of Surveying and Mapping 40(03): 85-89.

[8] Gao, K., Yang, H. B., Yin, H., Wang, W., Sun, Y., Zhao, L., Li, F. (2025): Estimating leaf water potential of potato using band-optimized spectral indices. – Journal of Irrigation and Drainage 44(03): 1-11.

http://www.aloki.hu ● ISSN 1589 1623 (Print) ● ISSN1785 0037 (Online)
DOI: http://dx.doi.org/10.15666/aeer/2304_78557871

[9] Guan, L., Zhang, X., Jian, Y. N., Zhang, Q. L. (2024): Response of Net Photosynthetic Rate of Larix gmelinii to Physiological and Ecological Factors in Different Phenophases. – Forest and Grassland Resources Research 2: 101-108.

[10] Han, P., Zhai, Y. P., Liu, W. H., Lin, H. R., An, Q. S., Zhang, J., Ding, S. G., Zhang, D. W., Pan, Z. Y., Nie, X. H. (2023): Dissection of Hyperspectral Reflectance to Estimate Photosynthetic Characteristics in Upland Cotton (*Gossypium hirsutum* L.) under Different Nitrogen Fertilizer Application Based on Machine Learning Algorithms. – Plants 12(3): 455-455.

[11] Huo, Y. Q., Ling, C. D., Sun, J. H., Cai, J. T., Hu, S. J. (2024): Intelligent detection of chlorophyll content in kiwifruit leaves based on hyperspectroscopy. – Journal of Chinese Agricultural Mechanization 45(12): 154-161.

[12] Jiang, F. C., Sun, H. Y., Wang, Y. Z., Yang, L., Zhang, J. H. (2015): Photosynthetic characteristics of apricot cultivars (*Prunus armeniaca*) in southern Xinjiang regions. – Agricultural Research in the Arid Areas 33(02): 102-105+175.

[13] Jing, Q. F., Zhu, L., Zhang, Y., Cheng, Y. L., Nie, H. J., Li, L. A. (2023): Response and adaptation of *Echinochloa crusgalli* to photoperiod. – Pratacultural Science 40(11): 2849-2859.

[14] Li, L. T., Wang, S. Q., Ren, T., Wei, Q. Q., Ming, J., Li, J., Li, X. S., Cong, R. H., Lu, J. W. (2018): Ability of models with effective wavelengths to monitor nitrogen and phosphorus status of winter oilseed rape leaves using in situ canopy spectroscopy. – Field Crops Research 215: 173-186.

[15] Li, X., Zhao, S. W., Bao, X. X., Wu, Y. J., Yang, Z. C. (2024): Effects of photoperiods on morphology, photosynthetic characters and carbohydrate of cucumber seedlings. – Journal of China Agricultural University 4: 164-172.

[16] Li, Y. M., Wang, H., Zhao, H. L., Zhang, L. G., Zhang, P. C. (2024): Prediction model for the water content of *Lyceum barbarum* tree canopy based on hyperspectral transformation. – Journal of Chinese Agricultural Mechanization 45(11): 165-171+188.

[17] Liang, X., Feng, Q., Yang, S., Gou, F. X. (2024): Severity classification of potato early blight in field based on hyperspectral and convolutional neural network. – Jiangsu Journal of Agricultural Sciences 40(10): 1854-1862.

[18] Liu, C., Peng, Y., Fang, S. H. (2020): Remote estimation of rice leaf net photosynthetic rate based on hyperspectral reflectance. – Journal of China Agricultural University 25(01): 56-65.

[19] Liu, S. T., Wang, S. B., Wang, R. H., Wang, L. H., Li, Q. Y., Zhang, Z. G., Zhao, Z. Z. (2024): Studies on the Dynamics of Phytochrome B and Photoperiod Key Genes in Early/Late Bolting Chinese Cabbage Lines. – Acta Agriculturae Boreali-Sinica 39(02): 11-18.

[20] Loukas, B., Newsome, S. D., Chen, F. H., Wang, H., Guilderson, T. P., Bettinger, R. L. (2009): Agricultural origins and the isotopic identity of domestication in northern China. – Proceedings of the National Academy of Sciences of the United States of America 106(14): 5523-8.

[21] Lü, W., Li, Y. H., Mao, W. B., Gong, X., Chen, S. G. (2017): Comparison of Estimation Methods for Net Photosynthetic Rate of Wheat's Flag Leaves Based on Hyperspectrum. – Journal of Agricultural Resources and Environment 34(06): 582-586.

[22] Luo, S. J., He, Y. B., Li, Q., Jiao, W. H., Zhu, Y. Q., Yu, J. K., Zhao, C., Xu, R. Y., Zhang, S. L., Xu, F., Su, J., Han, Z. C., Li, Z. (2020): Assessment of unified models for estimating potato leaf area index under water stress conditions across ground-based hyperspectral data. – Journal of Applied Remote Sensing 14(1): 014517.

[23] Sun, S. B., Du, H. Q., Li, P. H., Zhou, G. M., Xu, X. J., Gao, G. L., Li, X. J. (2016): Retrieval of leaf net photosynthetic rate of moso bamboo forests using hyperspectral remote sen-sing based on wavelet transform. – Chinese Journal of Applied Ecology 27(01): 49-58.

[24] Sun, Y. T., Yang, H. Y., Sun, A. Z., Mei, F., Yi, W. L. (2020): Hyperspectral estimation model for SPAD value of rice leaves. – Journal of Southern Agriculture 51(05): 1062-1069.

http://www.aloki.hu ● ISSN 1589 1623 (Print) ● ISSN1785 0037 (Online)
DOI: http://dx.doi.org/10.15666/aeer/2304_78557871

[25] Tang, Z. J., Zhang, W., Huang, X. Y., Xiang, Y. Z., Zhang, F. C., Chen, J. Y. (2024): Soybean Seed Yield Estimation Model Based on Ground Hyperspectral Remote Sensing Technology. – Transactions of the Chinese Society for Agricultural Machinery 1: 145-153+240.
[26] Thorp, K. R., Thompson, A. L., Herritt, M. T. (2024): Phenotyping cotton leaf chlorophyll via in situ hyperspectral reflectance sensing, spectral vegetation indices, and machine learning. – Frontiers in Plant Science 15: 1495593.
[27] Wang, D., Dian, Y. Y., Le, Y., Huang, C. B. (2016): Net Photosynthetic Rate Inversion Based on Hyperspectral Vegetation Indices. – Geography and Geo-Information Science 32(04): 42-48.
[28] Wang, J. J., Chen, L., Wang, H. G., Cao, X. N., Liu, S. C., Tian, X., Qin, H. B., Qiao, Z. J. (2019): Effects of Hyperspectral Prediction on Leaf Nitrogen Content and the Grain Protein Content of Broomcorn Millet. – Scientia Agricultura Sinica 52(15): 2593-2603.
[29] Wang, J. J., Wang, H. G., Cao, X. N., Chen, L., Liu, S. C., Tian, X., Qin, H. B., Qiao, Z. J. (2020): Comprehensive Evaluation of Photoperiod Sensitivity Based on Different Traits of Broomcorn Millet. – Scientia Agricultura Sinica 53(3): 474-485.
[30] Wang, Y., Xu, S. T., Yao, H. Y., Yang, K. J., Li, Y. H. (2020): Retrieval of flag leaf net photosynthetic rate of wheat using hyperspectral remote sensing based on wavelet transform. – Journal of Zhejiang Agricultural Sciences 61(10): 1979-1984.
[31] Wu, T. A., Zhang, W., Wu, S. Y., Cheng, M. H., Qi, L. S., Shao, G. C., Jiao, X. Y. (2023): Retrieving rice (*Oryza sativa* L.) net photosynthetic rate from UAV multispectral images based on machine learning methods. – Frontiers in Plant Science 13: 1088499.
[32] Yan, Z. M. (2023): Effects of Different Photoperiod Treatments on Photosynthetic Parameters of Millet. – Modern Agricultural Science and Technology 21: 16-19.
[33] Yan, Y. C., Nan, R., Mi, T. X., Song, Y. X., Shi, F. H., Liu, X. R., Wang, Y. Q., Sun, F. L., Xi, Y. J., Zhang, C. (2023): Rapid and Nondestructive Evaluation of Wheat Chlorophyll under Drought Stress Using Hyperspectral Imaging. – International Journal of Molecular Sciences 24(6): 5825-5825.
[34] Yao, N., You, H. T., Zhang, X. L., Reng, Y. Y., Liu, X. K., Zeng, X. Y. (2009): Research on the Photosynthesis of Under-Forest Ginseng Leaf. – Journal of Jilin Agricultural University 31(02): 119-124+130.
[35] Zhang, J., Sun, B., Yang, C. H., Wang, C. Y., You, Y. H., Zhou, G. S., Liu, B., Wang, C. F., Kuai, J., Xie, J. (2022): A novel composite vegetation index including solar-induced chlorophyll fluorescence for seedling rapeseed net photosynthesis rate retrieval. – Computers and Electronics in Agriculture 198: 107031.
[36] Zhang, K., Yan, F. F., Liu, P. (2024): The application of hyperspectral imaging for wheat biotic and abiotic stress analysis: A review. – Computers and Electronics in Agriculture 221: 109008.

http://www.aloki.hu ● ISSN 1589 1623 (Print) ● ISSN1785 0037 (Online)
DOI: http://dx.doi.org/10.15666/aeer/2304_78557871